

SUPPORTING INFORMATION

Fructose Drinking Promotes Gut Leakiness, Endotoxemia and Liver Fibrosis through CYP2E1-Mediated Oxidative and Nitritative Stress

Young-Eun Cho^{1#}, Do-Kyun Kim^{2#}, Wonhyo Seo³, Bin Gao³, Seong-Ho Yoo⁴, and
Byoung-Joon Song^{1*}

Supporting Materials and Methods

Cell culture

The human colonic carcinoma T84 cell line (ATCC, CCL-248) was purchased from the American Type Culture Collection. T84 cells were grown in a humidified incubator under 95% air and 5% CO₂ at 37 °C in Ham's F-12 medium, supplemented with 10% fetal bovine serum (FBS), 40 mg/ml of penicillin, 90 mg/ml of streptomycin, and 8 mg/ml of ampicillin. Confluent monolayer cells appeared 6–14 days after plating. T84 monolayer cells were exposed to 2.5 mM fructose in the absence or presence of the selective CYP2E1 inhibitor chlormethiazole (CMZ) (40 μM) or iNOS inhibitor 1400W (1 μM) for additional 24 h prior to harvest for subsequent analyses.

Human stellate LX2 cells grown in DMEM with 10% FBS and antibiotics were treated with 100 ng/ml LPS, 2.5 mM fructose, or LPS (100 ng/ml)+fructose (2.5 mM) for 24 h.⁽¹⁾ The primary mouse hepatic stellate cells (HSCs) were isolated by Optiprep and Percoll gradients (Sigma, St. Louis, MO) as described.^(2, 3) The primary HSCs, grown in a humidified incubator under 95% air and 5% CO₂ at 37 °C for 2 days, were treated with 100 ng/ml LPS, 2.5 mM fructose, or LPS (100 ng/ml)+fructose (2.5 mM) for additional 24 h.

Endotoxin assay

Plasma endotoxin levels were determined using the commercially available endpoint LAL Chromogenic Endotoxin Quantitation Kit with a concentration range of 0.015-1.2 EU/mL (Thermo Fisher Scientific, Waltham, MA), as previously described.⁽⁴⁾

Determination of plasma ROS

The amounts of plasma ROS were visualized with 2',7'-dichlorofluorescein diacetate (DCFH-DA, Thermo Fisher Scientific). Following incubation with DCFH-DA at 37°C for 20 min, the DCFH-DA fluorescence was then determined by the method, as recently described.⁽⁵⁾

Determination of plasma uric acid and alcohol

The amounts of plasma uric acid and alcohol were assessed by using a commercially available kit (Abcam and BioVision, respectively).

Triglyceride determination in liver

Hepatic triglyceride (TG) levels were assessed by using a commercially available kit (Thermo Fisher Scientific), as described.^(5, 6)

CYP2E1 activity assay

CYP2E1 activities as *p*-nitrophenol hydroxylase in the liver homogenates (20 µg of proteins) were measured, as described.⁽⁶⁾

Immunoblot analysis and immunoprecipitation

Parts of liver tissue and small intestine from each rat or mouse were homogenized with RIPA buffer. Protein concentrations were determined using the BCA Protein Assay Kit, and 50 µg of protein from the indicated samples were separated by SDS/PAGE and transferred to nitrocellulose membranes. These membranes were incubated with the respective rabbit polyclonal antibody against CYP2E1 (1:5,000 dilution; Abcam), p-JNK (1:1,000 dilution; Cell Signaling), 3-NT (1:5,000 dilution; Abcam), iNOS (1:5,000 dilution; Abcam), Sirt1 (1:1,000 dilution; Cell Signaling), p-Sirt1 (1:1,000 dilution; Cell Signaling), Acetyl-Histone 3 (1:1,000 dilution; Cell Signaling), PGC-1α (1:1,000 dilution; Santa Cruz), cleaved caspase-3 (1:1,000 dilution; Cell Signaling), TIMP-1 (1:1,000 dilution; Santa Cruz), COL-I (1:1,000 dilution; Santa Cruz), TGF-β (1:1,000 dilution; Santa Cruz), ZO-1 (1:5,000 dilution; Abcam), claudin-1 (1:1,000 dilution; Thermo-Fisher), claudin-4 (1:1,000 dilution; Thermo-Fisher), occludin (1:5,000 dilution; Abcam), or PER-2 (1:1,000 dilution; Thermo-Fisher). Respective mouse monoclonal antibody against JNK (1:1,000 dilution; Cell Signaling), Bax (1:1,000 dilution; Santa Cruz), β-catenin (1:1,000 dilution; Santa Cruz), E-cadherin (1:1,000 dilution; Santa Cruz), Plakoglobin (1:1,000 dilution; Santa Cruz), α-tubulin (1:1,000 dilution; Santa Cruz), Ubiquitin (1:1,000 dilution; Cell Signaling), α-SMA (1:5,000 dilution; Sigma), SREP-1 (1:1,000 dilution; Santa Cruz), TLR-4 (1:5,000 dilution; Abcam), CLOCK (1:1,000 dilution; Santa Cruz), or β-actin (1:10,000 dilution; Santa Cruz) was also used to detect the specific antigen target, as indicated. Specific rabbit polyclonal antibodies to PPARα were kindly provided by Dr. James P. Hardwick (Northeastern Ohio University College of Medicine). After washing the nitrocellulose membranes with phosphate buffered saline (PBS) three times at 10 min intervals, horseradish peroxidase (HRP)-conjugated donkey anti-rabbit or anti-mouse IgG (Santa Cruz) was used as the secondary antibody at 1:5,000 dilution. Relative protein images were determined by using HRP-conjugated secondary antibodies and ECL substrates (Thermo-Fishers). The intensities of the immunoreactive bands were quantified by densitometry using ImageJ software (National Institutes of Health).

Immunoprecipitation of liver or small intestinal proteins was carried out, as described previously.⁽⁵⁾ Briefly, 0.5 mg proteins of hepatic or small intestinal proteins equally pooled from individual rats of control or fructose-exposed group were incubated with the specific antibody to each indicated target protein (e.g., anti-Sirt1, anti-claudin-1, or anti-β-catenin)

followed by incubation with protein A/G-Sepharose for 4 h at 4°C with constant head-to-tail rotations. Sepharose beads were pre-blocked with 2% BSA in PBS before being used for immunoprecipitation. After incubation, proteins bound to Sepharose beads were washed twice with lysis buffer, four times with ice-cold PBS and mixed with 2x SDS-PAGE gel loading buffer. Immunoprecipitated proteins were resolved by SDS-PAGE for subsequent immunoblot analyses using the antibody to each target protein, as indicated.

Immunohistochemistry analysis

Immunohistochemical (IHC) staining of CYP2E1, iNOS, ZO-1, or E-cadherin was conducted on paraffin-embedded liver or gut slides incubated with the rabbit specific HRP/DAB (ABC) detection IHC kit (Abcam) according to the manufacturer's instructions, as recently described.⁽⁵⁾

TUNEL assay

Small intestine specimens were fixed overnight in 10% buffered formalin and embedded in paraffin. The ApopTag peroxidase in situ apoptosis detection kit (Millipore, Billerica, MA) was used to identify apoptotic enterocytes or hepatocytes by the TUNEL analysis, as recently described.⁽⁵⁾

Immunofluorescence and confocal microscopy

For detecting ZO-1 by immunofluorescence, T84 colonic cells were initially plated onto chamber slides. For detecting α -SMA by immunofluorescence, LX2 human hepatic stellate cells (HSCs) or primary mouse HSCs were initially plated onto chamber slides. The cells were fixed for 30 min at room temperature with 3.7% paraformaldehyde, directly added to the culture medium, and then washed twice with PBS for 15 min each. After washing the cells with PBS containing 0.3% Triton X-100, T84 cells were blocked with 1.5% (w/v) BSA solution in PBS for an additional 15 min. After removal of the blocking solution, T84 cells were incubated with anti-ZO-1 antibody at 4 °C overnight, as described.

⁽⁵⁾ LX2 cells or primary mouse HSCs were incubated with anti- α -SMA antibody at 4 °C overnight. For immunofluorescence detection, the cells were incubated with Alexa Fluor 488-labeled anti-rabbit secondary antibody (Thermo-Fisher). For nuclear staining, the cells were incubated with 1 mg/mL 4',6'-diamino-2-phenylindole (DAPI) for 5 min. The cells were washed and mounted with VECTASHIELD mounting medium (Vector Laboratories, Burlingame, CA). Fluorescence images were collected by using a confocal microscope (Carl Zeiss, Oberkochen, Germany).

Enzyme-linked immunosorbent assay (ELISA)

The levels of a cytokine or chemokine in the liver lysates from rats or mice were determined by using the respective ELISA kits for TNF- α (Abcam, Cambridge, United Kingdom) or MCP-1 (Abcam, Cambridge, United Kingdom) by following the manufacturers' protocols, as previously described.⁽⁵⁾

TEER and FITC-Dextran 4-kDa analysis

Colonic T84 cells were grown on collagen-coated polycarbonate membrane Transwell inserts with a surface area of 0.33 cm² and 0.4 μ m pore size (Thermo Fisher Scientific). After a trans-epithelial electrical resistance (TEER) 600 Ohm·cm² was developed, monolayer T84 cells were exposed to 2.5 or 5.0 mM fructose either alone or pretreated with a CYP2E1 inhibitor or an iNOS inhibitor for 1 h. TEER of epithelial monolayers was measured after incubation for 24 h with an epithelial volt-ohm-meter in each insert and multiplied by the membrane surface area (0.33 cm²), corrected by subtracting background resistance of the blank membrane (i.e., no cells). Data were collected from duplicate inserts per treatment in three experiments and expressed as percentage of basal TEER (i.e., 600 Ohm·cm²) obtained before treatment.

At the end of TEER measurements, FITC-labeled 4-kDa dextran (1 mg/ml FITC-D4, Sigma-Aldrich, St. Louis, MO) was added to the apical side of cells and incubated for 1 h at 37°C. Monolayer permeability was assessed by measuring the fluorescence of FITC-

D4 in the basal medium compartment spectrophotometrically using a microplate reader at excitation and emission spectra of 485 nm and 540 nm, respectively. Data were reported as relative fluorescent units (% baseline).

***In vivo* permeability measurement by using FITC-D4**

Intestinal permeability was determined by using a protocol previously described.^(7, 8) In brief, WT mice exposed to water or fructose in drinking water for 8 weeks (n=7~8/group) were fasted for 6 hours and treated with FITC-D4 (600 mg/kg via oral gavage) (Sigma-Aldrich) from a solution (250 mg/mL). One hour later, 120 μ L blood was collected, stored on ice in the dark and centrifuged at 12,000 x g for 3 mins. The supernatant plasma was transferred into a clean tube and then diluted 1:2 in PBS before the concentration of FITC-D4 determined by fluorescence spectroscopy (excitation at 485 nm and emission at 535 nm) relative to a linear standard curve prepared with the diluted FITC-D4 solutions in plasma from untreated mice.

Caspase activity measurement

Caspase activities were measured by using Caspase-Glo 3/7 assay kits (Promega Corp, Madison, WI) by following the manufacturer's protocols, as described.⁽⁵⁾

Hepatic non-parenchymal cell preparation

For liver macrophage analysis, non-parenchymal cells were prepared by collagenase digestion and fractionation on a two-step Percoll density gradient, as previously described.⁽⁹⁾

RNA extraction and Real-time analysis

Total RNA was extracted from the liver and non-parenchymal cells of each animal using Trizol (Thermo Fisher Scientific), as previously described.⁽⁵⁾ For real-time analysis, cDNA was transcribed from a total of 600 ng of DNase I-treated RNA using the cDNA reverse-transcription kit and random primers. Quantitative real-time reverse-transcriptase polymerase chain reaction (qRT-PCR) was performed using a Mx3000p System. To determine relative mRNA expression, house-keeping gene (β -actin) and apoptosis marker gene with SYBR green I (SYBR Advantage qPCR Premix) were used. The sequences of forward and reverse primers for each target gene are listed in **Supporting Table 2**. CLOCK and PER-2 primers were purchased from Qiagen: *clock* (rat Cat No. PPR49736B; mice Cat No. PPM24994A) and *PER-2* (rat Cat No. PPR48062A; mice Cat No. PPM25497F).

16S sequencing and bioinformatics

Stool samples were aseptically collected from the cecum of each rat and rapidly frozen at -80°C . DNA was extracted using Mag-Bind Universal Pathogen DNA Kit (Omega Bio-Tek, Norcross, GA) following the manufacturer's protocols. DNA sequencings for bacterial 16S ribosomal V3-V4 region of each stool sample were performed at the Omega Bioservices Inc. (www.omegabioservices.com). The 16S ribosomal V3-V4 regions were amplified using the following primers: F: 5'-CCTACGGGNGGCWGCAG-3' and R: 5'-GACTACHVGGGTATCTAATCC-3'. Sequence data was processed with Qiime 2 against the Greengenes 13.8 database to assign taxonomy.

Statistical analysis

Statistical significance was determined using two-tailed t-test; ANOVA and Dunnet's multiple comparison post-test were used to compare the means of multiple groups. Data shown as mean \pm SD and were considered statistically significant at $p < 0.05$. GraphPad Prism 7.0 (GraphPad Software Inc., La Jolla, CA) was used for analysis. Other methods not described here were the same, as previously described.^(4, 5)

References

1. Liu M, Xu Y, Han X, Yin L, Xu L, Qi Y, Zhao Y, et al. Dioscin alleviates alcoholic liver fibrosis by attenuating hepatic stellate cell activation via the TLR4/MyD88/NF-kappaB signaling pathway. *Sci Rep* 2015;5:18038.
2. Ramirez T, Li YM, Yin S, Xu MJ, Feng D, Zhou Z, Zang M, et al. Aging aggravates alcoholic liver injury and fibrosis in mice by downregulating sirtuin 1 expression. *J Hepatol* 2017;66:601-609.
3. Seo W, Eun HS, Kim SY, Yi HS, Lee YS, Park SH, Jang MJ, et al. Exosome-mediated activation of toll-like receptor 3 in stellate cells stimulates interleukin-17 production by gammadelta T cells in liver fibrosis. *Hepatology* 2016;64:616-631.
4. Cho YE, Song BJ. Pomegranate prevents binge alcohol-induced gut leakiness and hepatic inflammation by suppressing oxidative and nitrate stress. *Redox Biol* 2018;18:266-278.
5. Cho YE, Yu LR, Abdelmegeed MA, Yoo SH, Song BJ. Apoptosis of enterocytes and nitration of junctional complex proteins promote alcohol-induced gut leakiness and liver injury. *J Hepatol* 2018;69:142-153.
6. Cho YE, Mezey E, Hardwick JP, Salem N, Jr., Clemens DL, Song BJ. Increased ethanol-inducible cytochrome P450-2E1 and cytochrome P450 isoforms in exosomes of alcohol-exposed rodents and patients with alcoholism through oxidative and endoplasmic reticulum stress. *Hepatol Commun* 2017;1:675-690.
7. Cani PD, Bibiloni R, Knauf C, Waget A, Neyrinck AM, Delzenne NM, Burcelin R. Changes in gut microbiota control metabolic endotoxemia-induced inflammation in high-fat diet-induced obesity and diabetes in mice. *Diabetes* 2008;57:1470-1481.
8. Johnson AM, Costanzo A, Gareau MG, Armando AM, Quehenberger O, Jameson JM, Olefsky JM. High fat diet causes depletion of intestinal eosinophils associated with intestinal permeability. *PLoS One* 2015;10:e0122195.
9. Nnalue NA, Shnyra A, Hultenby K, Lindberg AA. *Salmonella choleraesuis* and *Salmonella typhimurium* associated with liver cells after intravenous inoculation of rats are localized mainly in Kupffer cells and multiply intracellularly. *Infect Immun* 1992;60:2758-2768.

Supporting Table S1. Effect of fructose drinking on food intake, weight gain, and liver weight in rats or mice.

A. Rats

	Water	Fructose
Liquid intake (in mL/day)	20 ± 3	34 ± 4**
Chow intake (in g/day)	11.9 ± 0.6	7.8 ± 0.8**
Weight gain (g)	218.0 ± 5.9	230.5 ± 1.5
Liver weight (in g)	6.3 ± 0.1	8.8 ± 0.3**
Liver to body weight ratio (%)	2.9 ± 0.1	3.8 ± 0.2**

Data represent means ± SEM (n=8 or 10/group). ***P* < 0.01.

B. Mice

	Wide type mice		<i>Cyp2e1</i>-null mice	
	Water	Fructose	Water	Fructose
Liquid intake (in mL/day)	4.6 ± 0.2	4.1 ± 0.3	4.9 ± 0.6	5.8 ± 0.4
Chow intake (in g/day)	2.7 ± 0.3	3.4 ± 0.4	2.1 ± 0.3	2.6 ± 0.5
Weight gain (g)	21.7 ± 0.7	22.7 ± 0.6	20.0 ± 0.6	21.8 ± 0.7
Liver weight (in g)	0.7 ± 0.06	1.0 ± 0.05*	0.8 ± 0.07	0.9 ± 0.04
Liver to body weight ratio (%)	3.2 ± 0.3	4.3 ± 0.2*	3.8 ± 0.3	3.9 ± 0.3

Data represent means ± SEM (n=6/group). **P* < 0.05, ***P* < 0.01.

Supporting Table S2. Sequences of oligonucleotide primers used in real-time PCR.

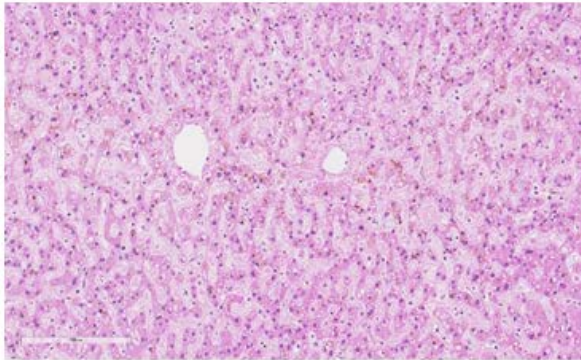
Gene	Sequence (5' - 3')
Rats	
MCP-1	F: 5'-AGCATCCACGTGCTGTCTC-3' R: 5'-GATCATCTTGCCAGTGAATGAG-3'
TNF α	F: 5'-CGAGTGACAAGCCCGTAGCC-3' R: 5'-GGATGAACACGCCAGTCGCC-3'
IL-6	F: 5'-TGCCAACCTTGTGGTATCAGCCA-3' R: 5'-TGAAGACACAGAGAAGCAATCC-3'
ARG-1	F: 5'-AAAGCCCATAGAGATTATCGGAGCG-3' R: 5'-AGACAAGGTCAACGGCACTGCC-3'
PGC1 α	F: 5'-ATGAGAAGCGGGAGTCTG AA-3' R: 5'-ACGGTGCATTAATCAATTTTC-3'
PPAR α	F: 5'-ACGATGCTGTCCTCCTTGATG-3' R: 5'-ACGGTGCATTAATCAATTTTC-3'
α SMA	F: 5'-CCGAGATCTCACCGACTACC-3' R: 5'-TCCAGAGCGACATAGCACAG-3'
TGF β 1	F: 5'-ACCGCAACAACGCAATCTATG-3' R: 5'-TTCCGTCTCCTTGGTTCAGC-3'
<i>E. coli</i>	F: 5'-GTTAATACCTTTGCTCATTGA-3' R: 5'-ACCAGGGTATCTAATCCTGTT-3'
GAPDH	F: 5'-ACCACAGTCCATGCCATCAC-3' R: 5'-TCCACCACCCTGTTGCTGTA-3'
Mice	
NLRP3	F: 5'-TGCTCTTCACTGCTATCAAGCCCT-3' R: 5'-ACAAGCCTTTGCTCCAGACCCTAT-3'
IL-1 β	F: 5'-GGAGAACCAAGCAACGACAAAATA-3' R: 5'-TGGGGAACTCTGCAGACTCAAAC-3'
TNF α	F: 5'-TGGCCAGACCCTCACACTCAG-3' R: 5'-ACCCATCGGCTGGCACCCT-3'
<i>E. coli</i>	F: 5'-CATTGACGTTACCCGCAGAAGAAGC-3' R: 5'-CTCTACGAGACTCAAGCTTGC-3'
GAPDH	F: 5'-ATGGTGAAGGTCGGTGTG-3' R: 5'-CATTCTCGGCCTTGACTG-3'

SUPPORTING FIGURES

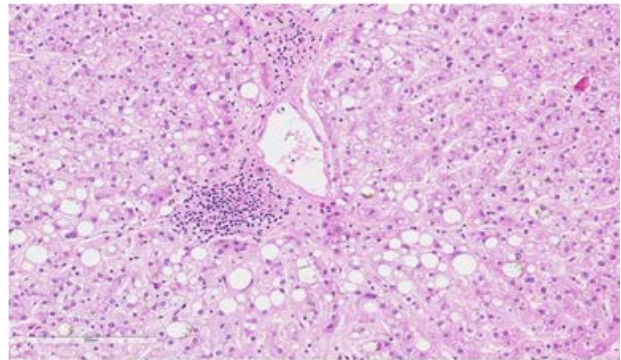
Supporting Fig. S1

H&E staining of autopsied human livers

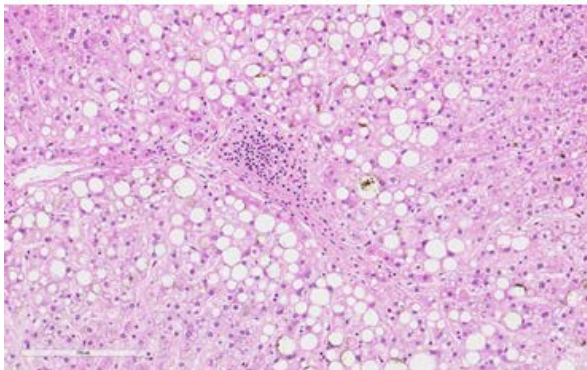
Control



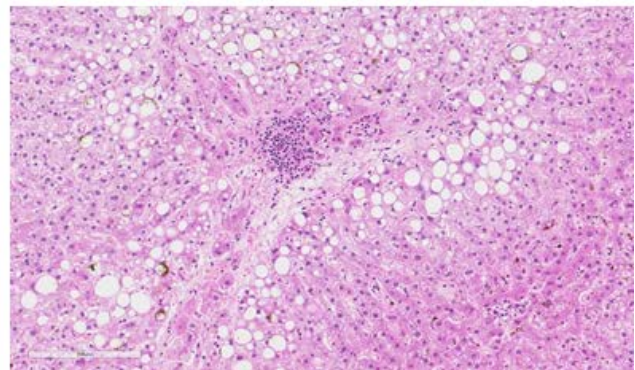
NASH-1



NASH-2



NASH-3

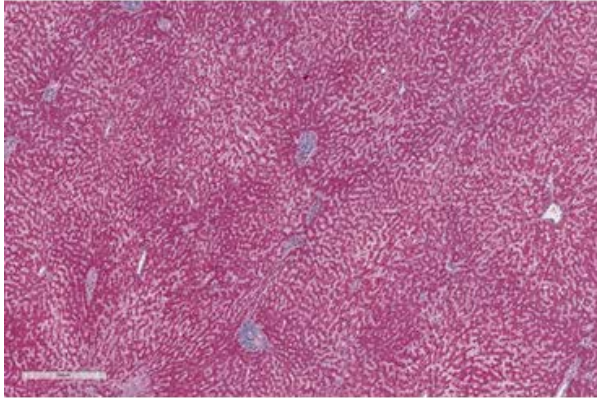


Supporting Fig. S1. Hematoxylin-eosin-stained liver sections for non-obese (CON) versus obese (NASH) people.

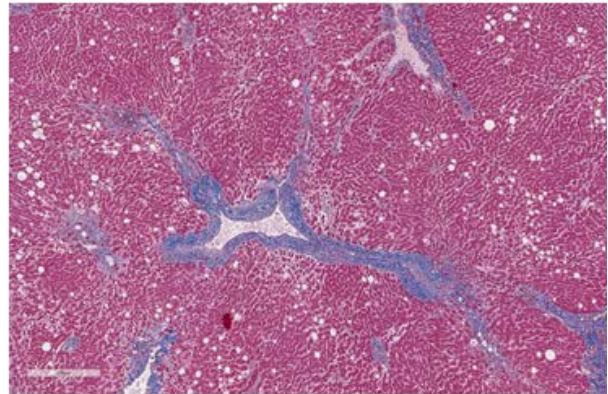
Supporting Fig. S2

Masson's trichrome staining of autopsied human livers

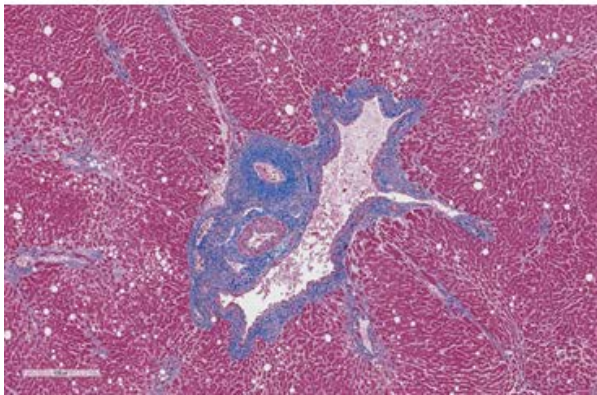
Control



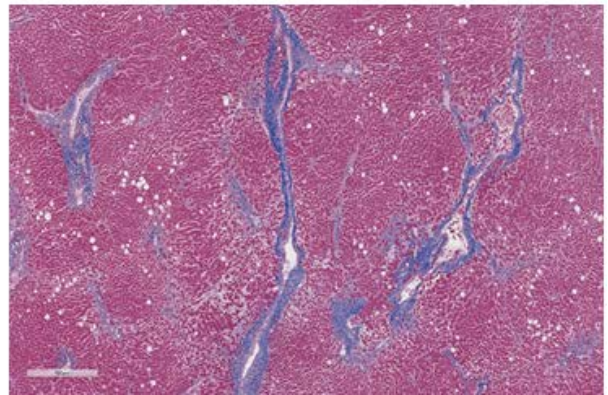
NASH-1



NASH-2



NASH-3



Supporting Fig. S2. Masson's trichrome-stained liver sections for non-obese (CON) versus obese (NASH) people.

Supporting Fig. S3

H&E staining of rat colons

Water

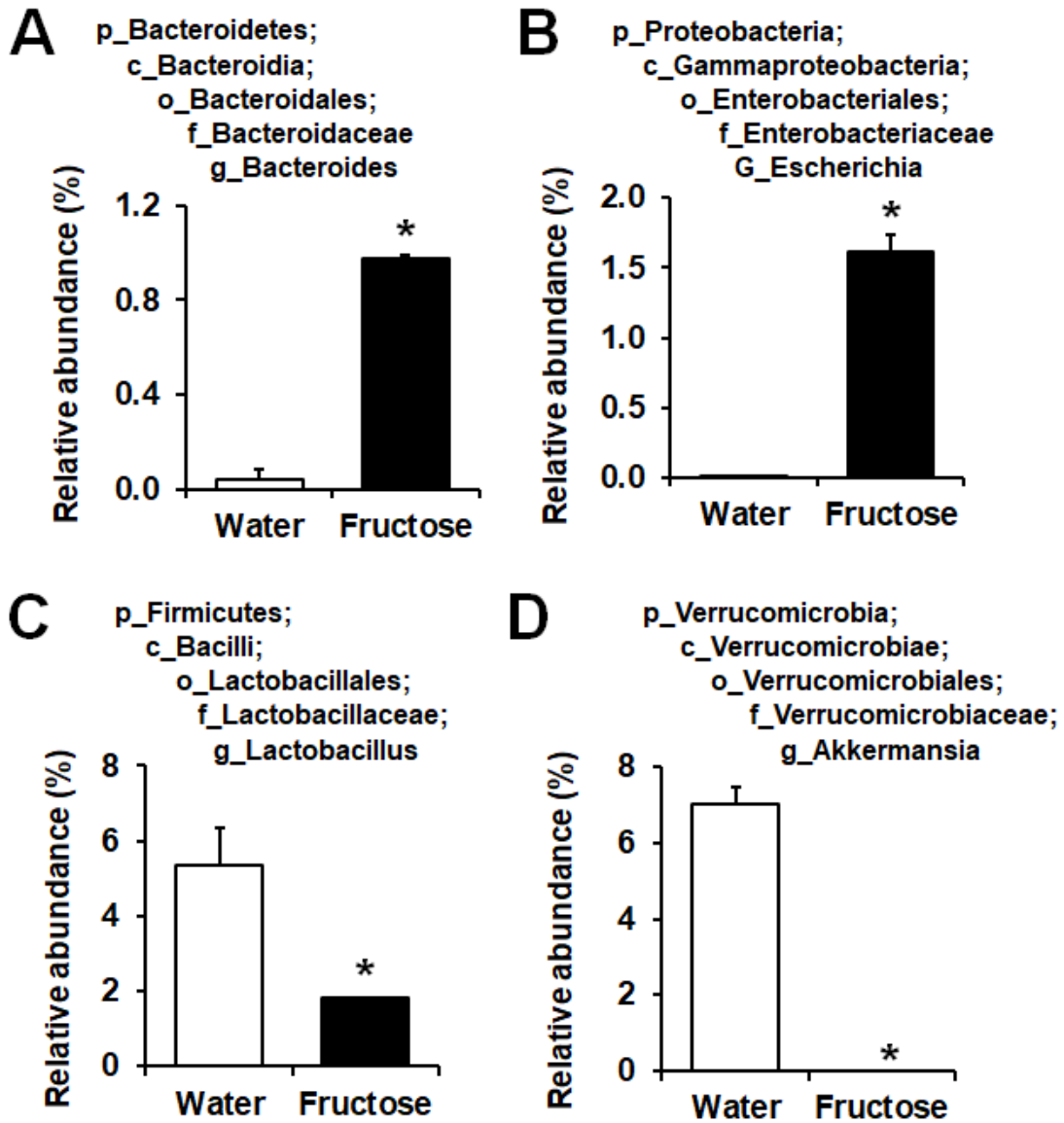


Fructose



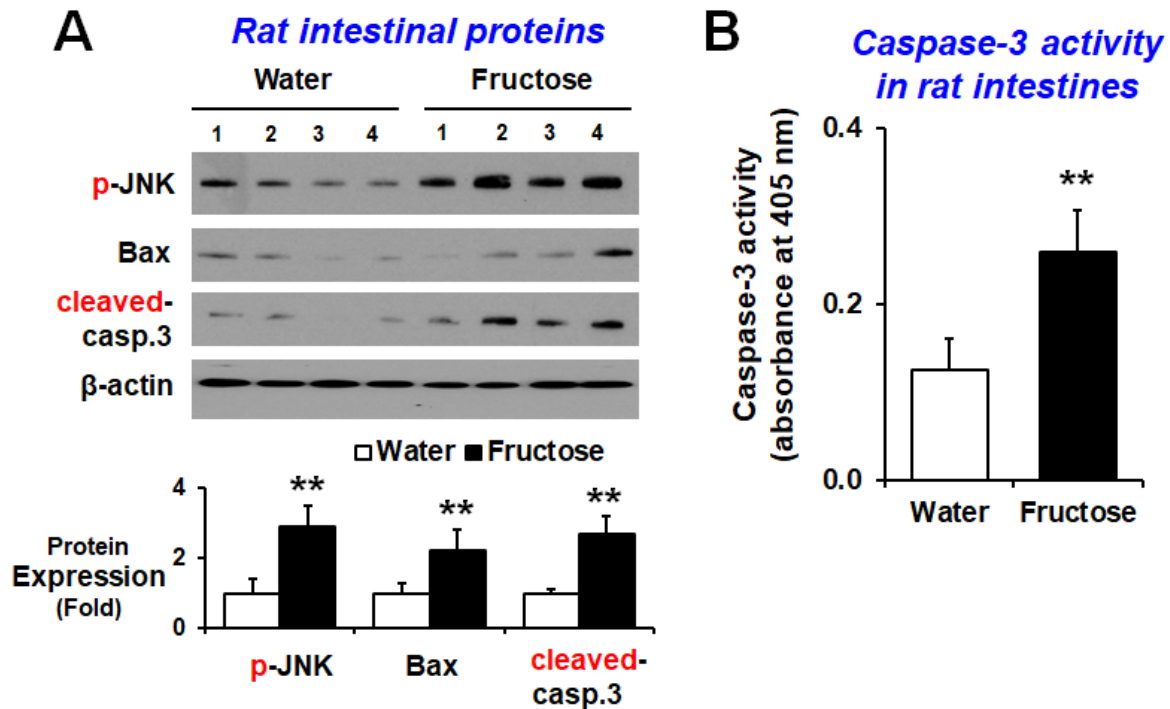
Supporting Fig. S3. Histological evaluation of rat colons. Representative H&E stained slides for microscopic evaluation of colon sections from the water-control and fructose-exposed groups.

Supporting Fig. S4



Supporting Fig. S4. Fructose exposure changed gut microbiota composition. (A-D) The *Bacteroides* (A), *Enterobacteriaceae* (B), *Lactobacillus* (C) and *Akkermansia* (D) exhibited significant differences between the water-control and fructose-exposed groups. Data represent means \pm SD (n=3~4/group) where statistical significance was determined using two-tailed t-test: * $P < 0.05$; ** $P < 0.01$.

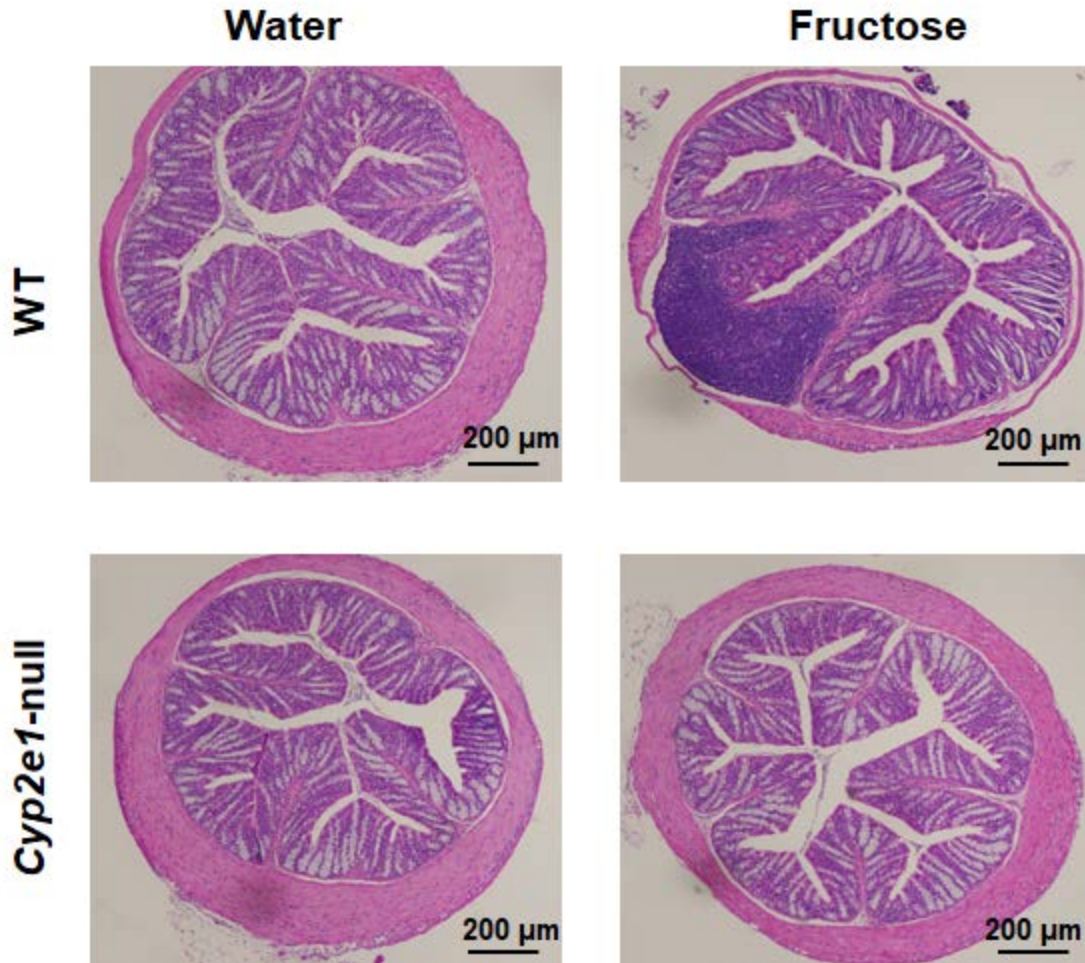
Supporting Fig. S5



Supporting Fig. S5. Fructose promoted apoptosis marker proteins and caspase 3 activity in rats. (A) The levels of liver apoptosis marker proteins p-JNK, Bax, and cleaved-caspase-3 in the indicated rat groups are presented. Densitometric quantitation of each immunoreactive protein relative to β -actin, used as a loading control, is shown (n=8/group). (B) Caspase-3 activity (n=8/group). Data represent means \pm SD where statistical significance was determined using two-tailed t-test: ** P <0.01.

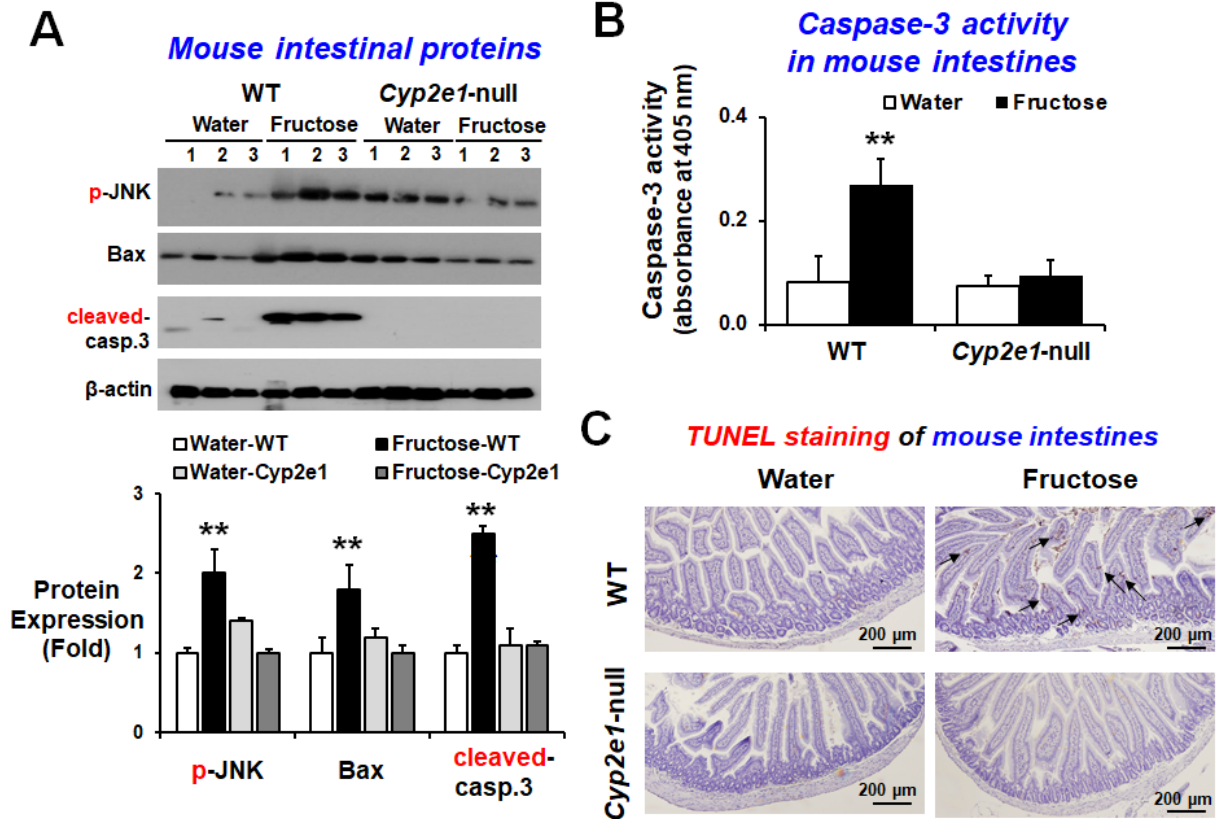
Supporting Fig. S6

H&E staining of mouse colons



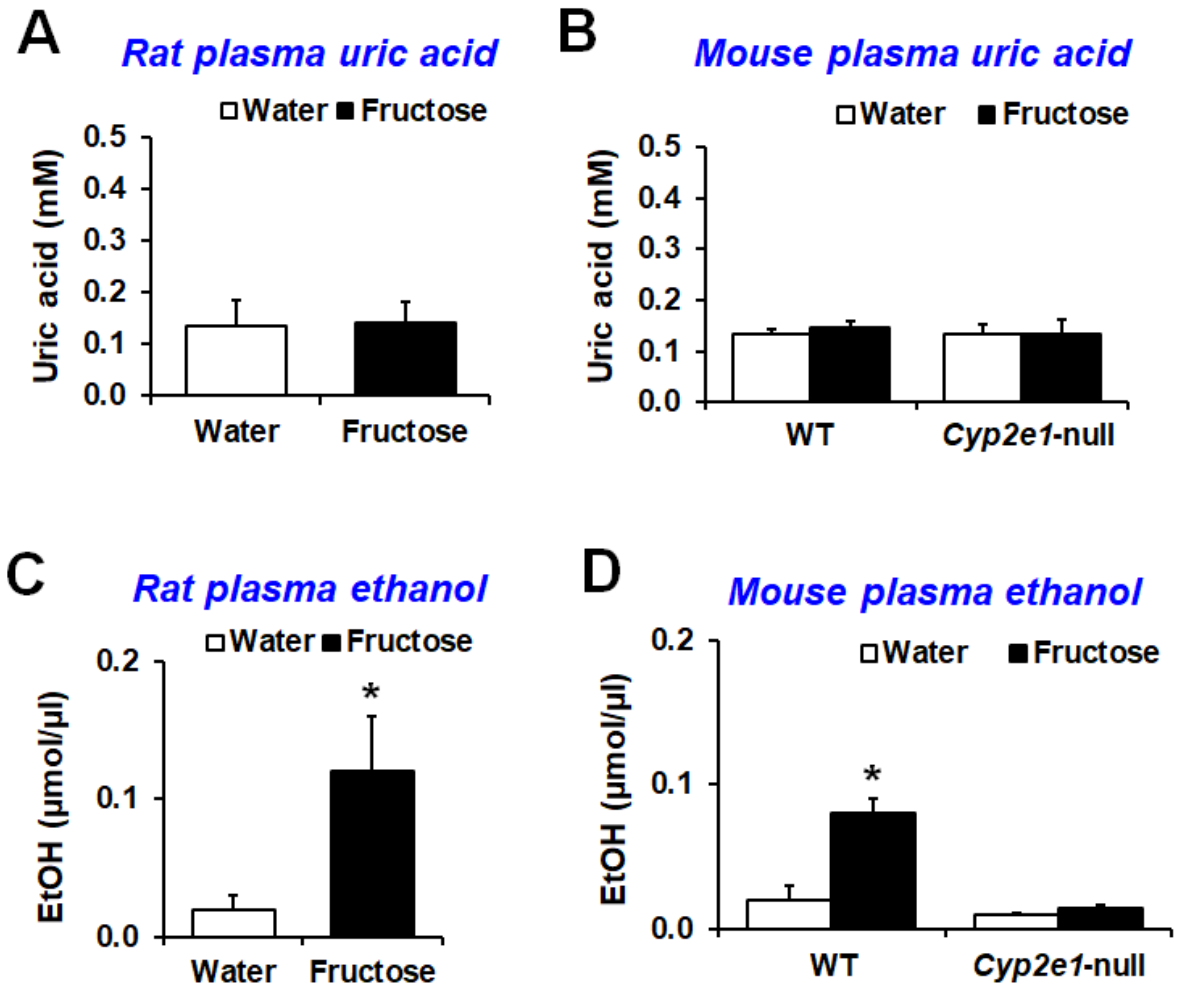
Supporting Fig. S6. Histological evaluation of mouse colons. Representative H&E stained slides for microscopic evaluation of colon sections in the indicated mouse groups.

Supporting Fig. S7



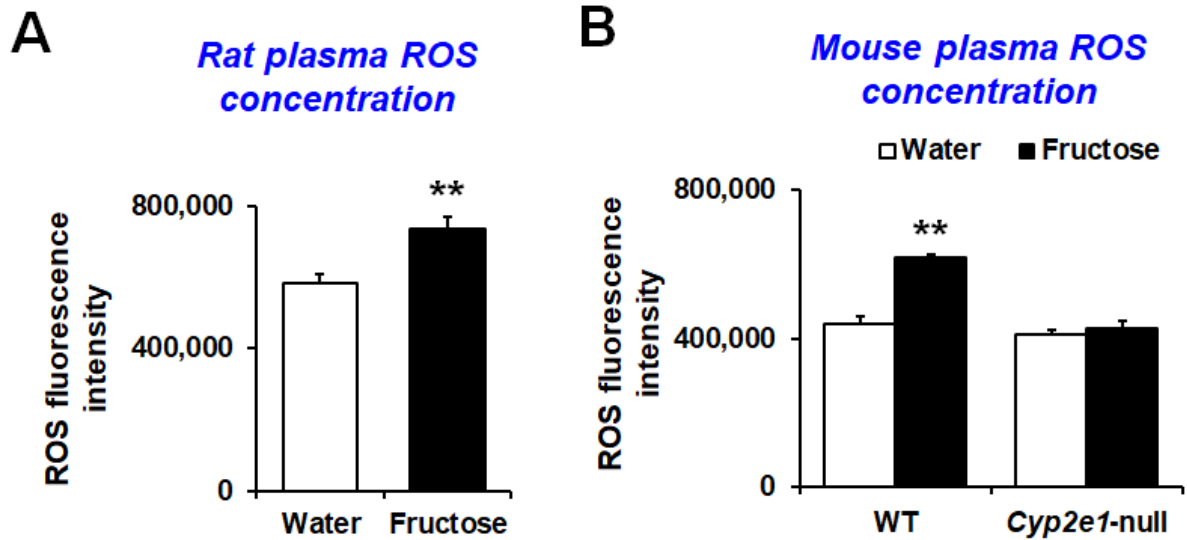
Supporting Fig. S7. Fructose promoted apoptosis marker proteins and caspase 3 activity in WT mice, but not in the *Cyp2e1*-null mice. (A) The levels of liver apoptosis marker proteins p-JNK, Bax, and cleaved-caspase-3 in the indicated mouse groups are presented. Densitometric quantitation of each immunoreactive protein relative to β -actin, used as a loading control, is shown ($n=6$ /group). (B) Caspase-3 activity ($n=6$ /group). Data represent means \pm SD where statistical significance was determined using two-tailed t-test: ** $P<0.01$. (C) Representative TUNEL staining for apoptotic enterocytes (arrows) in the indicated mouse groups.

Supporting Fig. S8



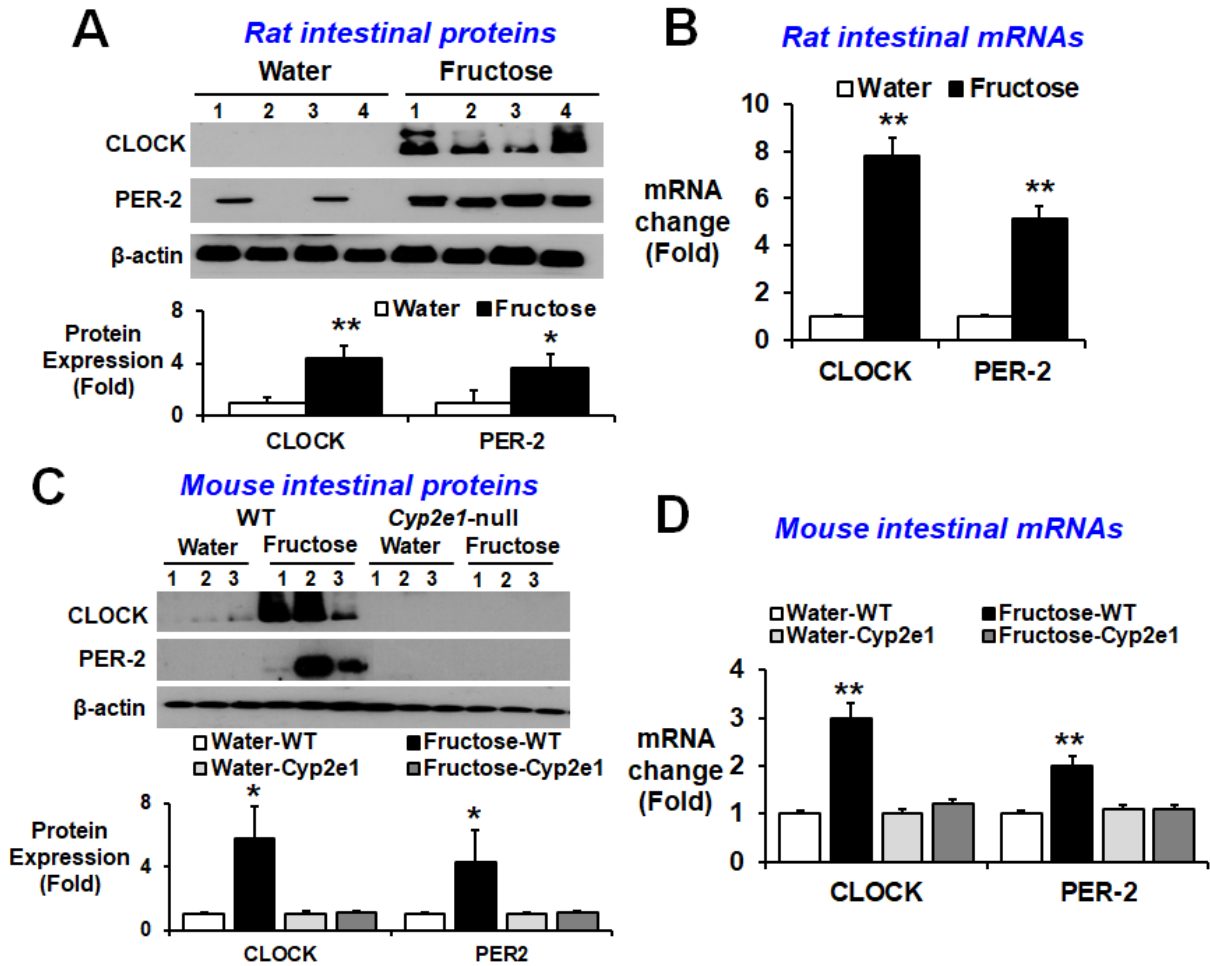
Supporting Fig. S8. Elevated plasma ethanol concentration without change in uric acid concentration in the fructose-exposed rats or WT mice but not in the corresponding *Cyp2e1*-null mice. Data represent means \pm SD where statistical significance was determined using two-tailed t-test: * $P < 0.05$.

Supporting Fig. S9



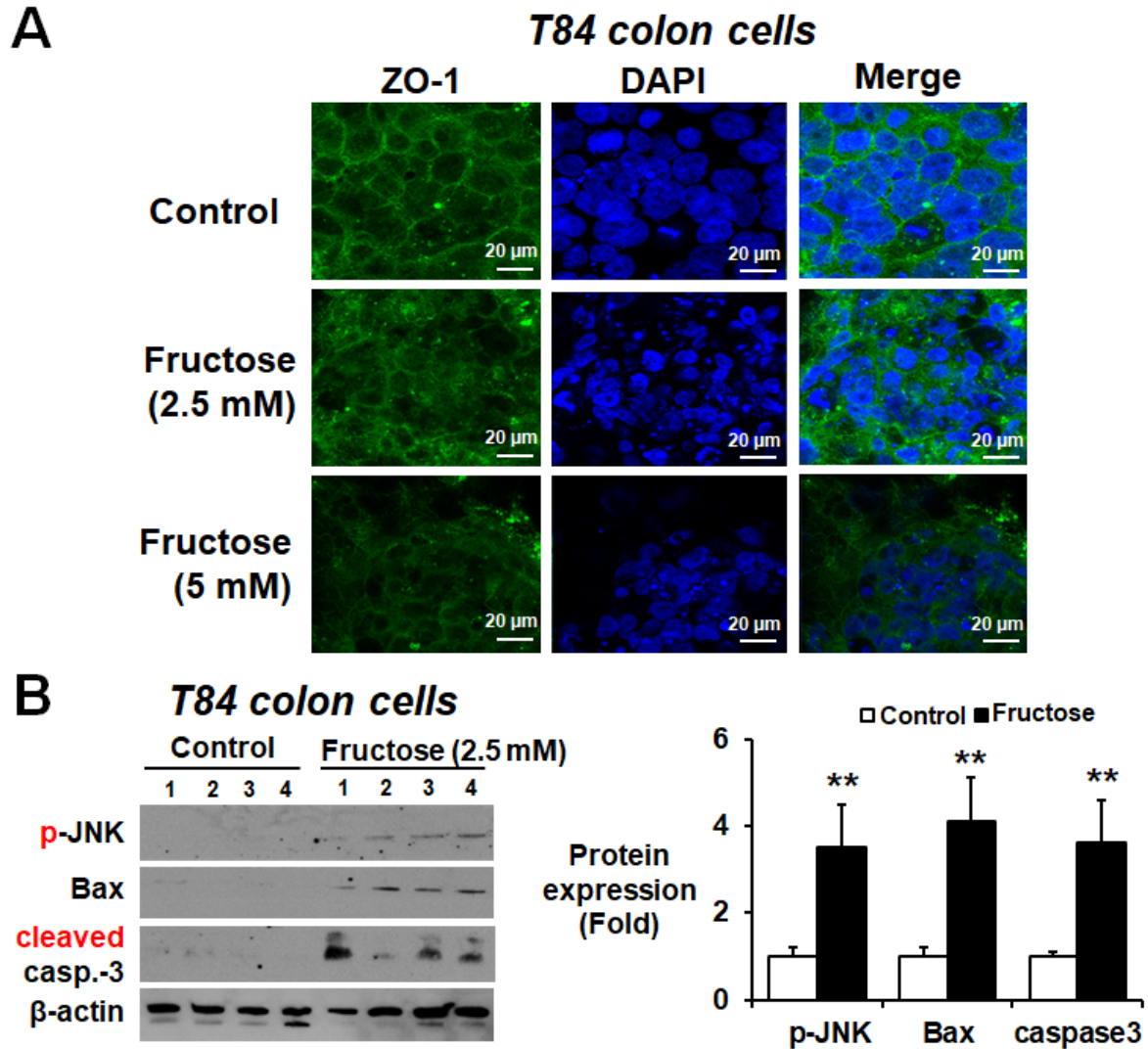
Supporting Fig. S9. Fructose drinking increased plasma ROS levels in rats or WT mice but not in the corresponding *Cyp2e1*-null mice. Data represent means \pm SD where statistical significance was determined using two-tailed t-test: ** $P < 0.01$.

Supporting Fig. S10



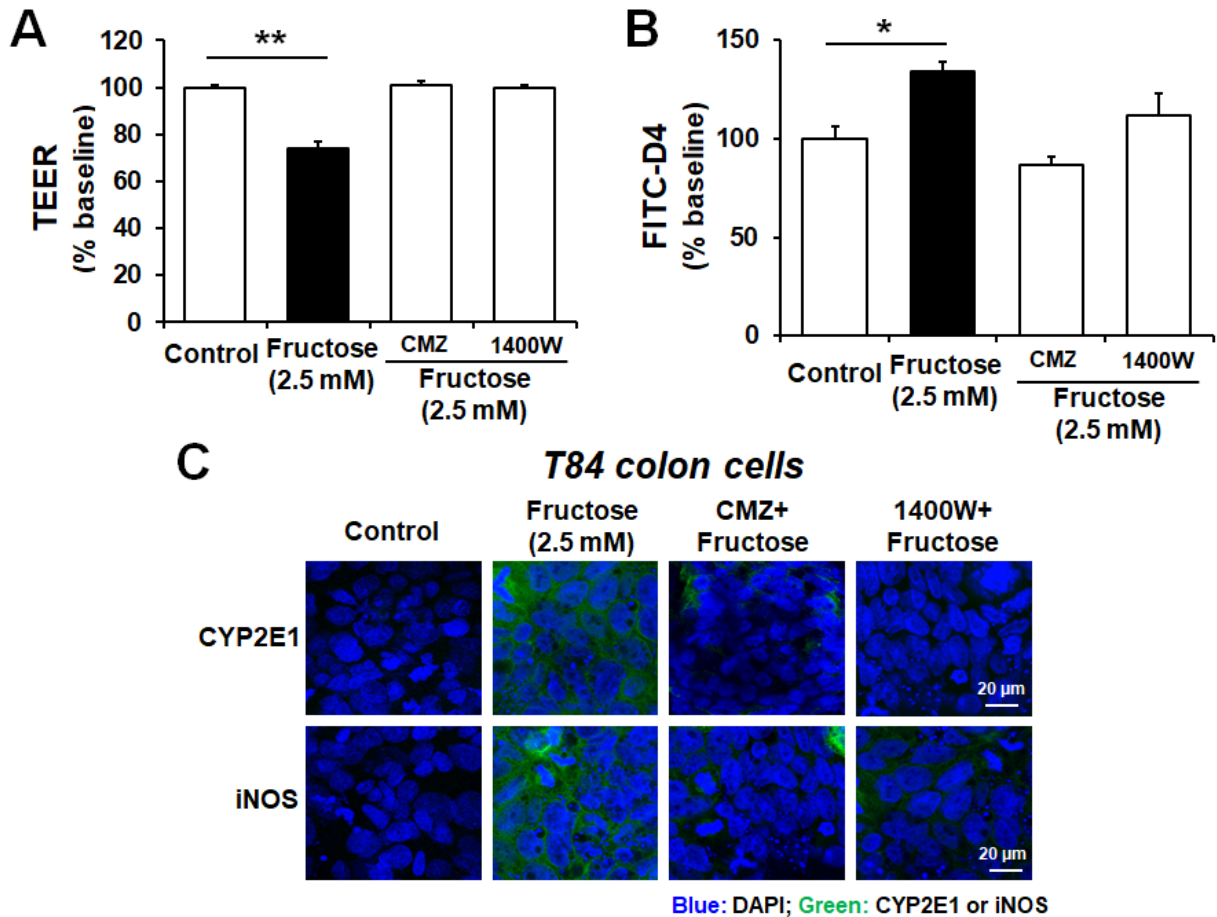
Supporting Fig. S10. Fructose drinking increased CLOCK and PER-2 mRNAs and proteins in rats or WT mice but not in the corresponding *Cyp2e1*-null mice. Immunoblots results for the hepatic levels of CLOCK and PER-2 proteins in the indicated mouse groups are presented. Densitometric quantitation of each immunoreactive protein relative to β -actin, used as a loading control, is shown ($n=6$ /group). Data represent means \pm SD where statistical significance was determined using two-tailed t-test: * $P < 0.05$; ** $P < 0.01$.

Supporting Fig. S11



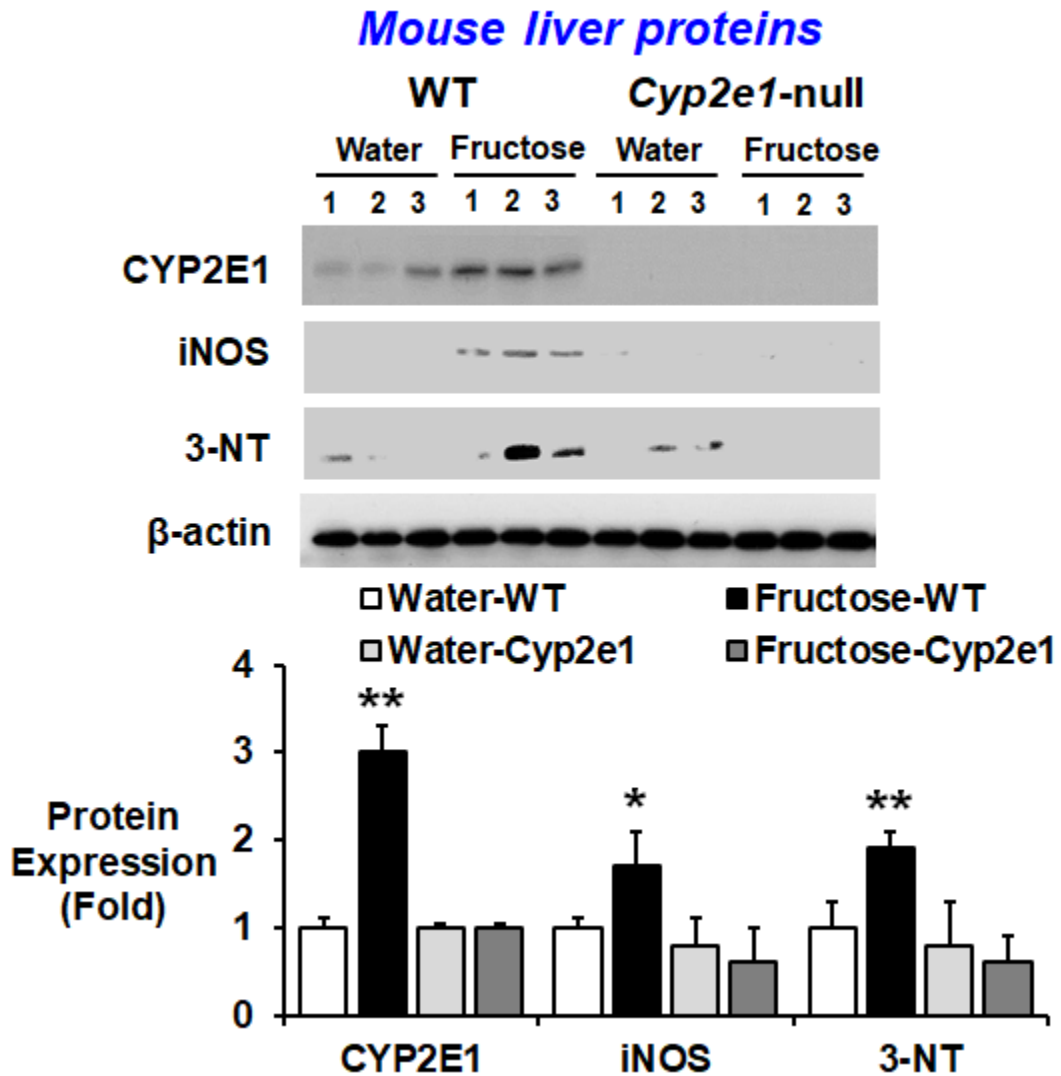
Supporting Fig. S11. Fructose disrupted the distribution of the tight junction protein ZO-1 and increased the levels of apoptosis marker proteins in T84 colon cells. (A) The confocal image shows disorganization of ZO-1 in T84 cells after treatment with the indicated concentrations of fructose for 24 h. Nuclei of T84 cells were counterstained with DAPI. (B) Immunoblot results for apoptosis marker proteins phospho-JNK, Bax, or cleaved-caspase3 in T84 cells and densitometric quantitation for each protein relative to β -actin, used as a loading control, are shown from the indicated groups. ** $P < 0.01$.

Supporting Fig. S12



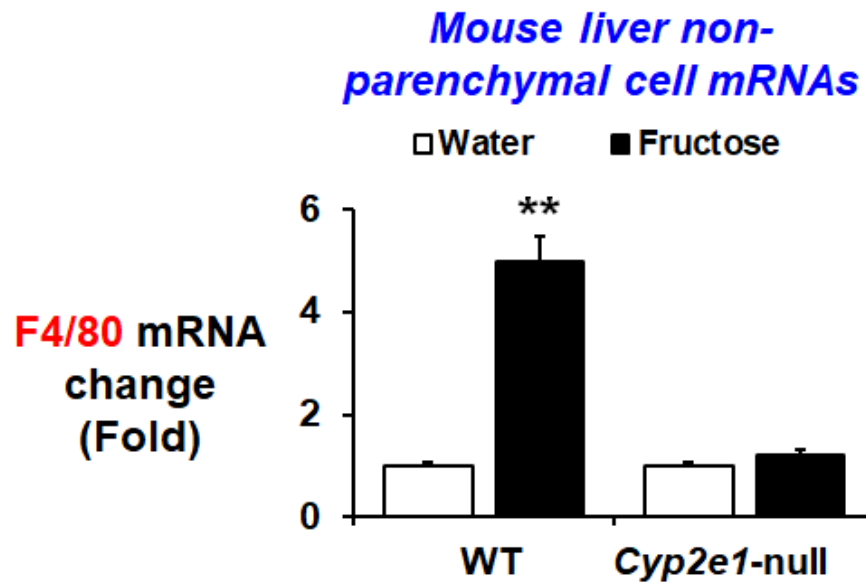
Supporting Fig. S12. CYP2E1 and iNOS play an important role in regulating fructose-induced epithelial cell barrier dysfunction in T84 colonic cells. (A and B) T84 cells were treated with culture media (CON) or 2.5 mM fructose for 24 h, as indicated. Representative levels of trans-epithelial electrical resistance (TEER) and permeability to FITC-D4 after 1 h treatment with the specific CYP2E1 inhibitor chlormethiazole (CMZ, 40 μ M) or an iNOS inhibitor 1400W (1 μ M), respectively. Permeability is expressed as percentage of basal TEER and FITC-D4 permeation from apical side of T84 cells to basal chamber. Data represent means \pm SD of triplicate wells from two separate experiments. * $P < 0.05$; ** $P < 0.01$. (C) The confocal images show the changed amounts and disorganization of CYP2E1 or iNOS in fructose-exposed T84 cells after treatment with the indicated inhibitor of CYP2E1 or iNOS for 24 h.

Supporting Fig. S13



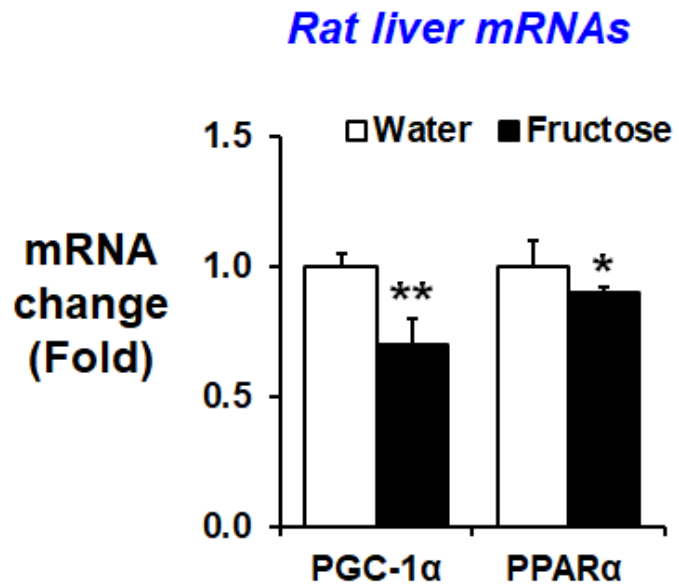
Supporting Fig. S13. Fructose drinking increased nitroxidative stress marker proteins in WT mice but not in *Cyp2e1*-null mice. Immunoblots results for the hepatic levels of nitroxidative stress marker proteins CYP2E1, iNOS, and nitrated proteins in the indicated mouse groups are presented. Densitometric quantitation of each immunoreactive protein relative to β -actin, used as a loading control, is shown (n=6/group). Data represent means \pm SD where statistical significance was determined using two-tailed t-test: * $P < 0.05$; ** $P < 0.01$.

Supporting Fig. S14



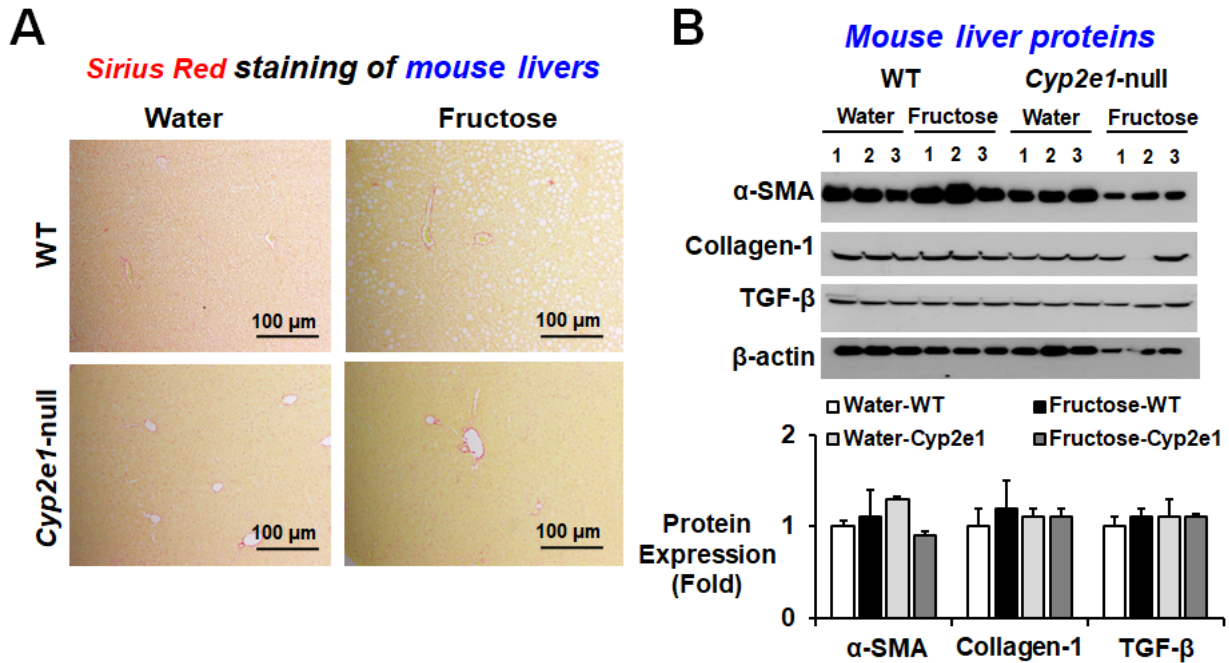
Supporting Fig. S14. Fructose exposure changed the mRNA of F4/80 in mouse liver non-parenchymal cells. ** $P < 0.01$.

Supporting Fig. S15



Supporting Fig. S15. Fructose drinking significantly decreased the hepatic PGC1- α and PPAR α mRNA expression. * $P < 0.05$; ** $P < 0.01$.

Supporting Fig. S16



Supporting Fig. S16. Fructose drinking did not change the hepatic fibrosis markers in WT mice or *cyp2e1* null mice. (A) Representative Sirius red staining of formalin-fixed liver sections for the indicated mouse groups. (B) Immunodetection of the hepatic fibrosis marker proteins (α -SMA, collagen-1, and TGF- β) in the indicated groups. Densitometric quantitation of the immunoblot for each protein relative to β -actin, used as a loading control, is shown.